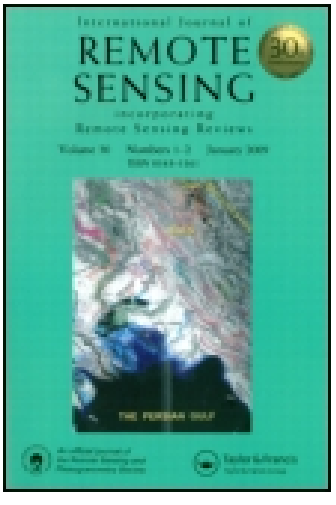

International Journal of Remote Sensing
Publication details, including instructions for authors and subscription information:
http://www.tandfonline.com/loi/tres20

Saharan dust as a causal factor of hemispheric asymmetry in aerosols and cloud cover over the tropical Atlantic Ocean

Pavel Kishcha[a], Arlindo da Silva[b], Boris Starobinets[a], Charles Long[c], Olga Kalashnikova[d] & Pinhas Alpert[a]

[a] Department of Geosciences, Tel-Aviv University, Tel-Aviv 69978, Israel

[b] Global Modeling and Assimilation Office, NASA/GSFC, Code 610.1, Greenbelt, MD 20771, USA

[c] Pacific Northwest National Laboratory, P.O. Box 999, Richland, WA, USA

[d] Jet Propulsion Laboratory, California Institute of Technology, Pasadena, CA 91109, USA

Published online: 09 Jul 2015.

To cite this article: Pavel Kishcha, Arlindo da Silva, Boris Starobinets, Charles Long, Olga Kalashnikova & Pinhas Alpert (2015) Saharan dust as a causal factor of hemispheric asymmetry in aerosols and cloud cover over the tropical Atlantic Ocean, International Journal of Remote Sensing, 36:13, 3423-3445, DOI: 10.1080/01431161.2015.1060646

To link to this article: http://dx.doi.org/10.1080/01431161.2015.1060646

International Journal of Remote Sensing, 2015
Vol. 36, No. 13, 3423–3445, http://dx.doi.org/10.1080/01431161.2015.1060646

Saharan dust as a causal factor of hemispheric asymmetry in aerosols and cloud cover over the tropical Atlantic Ocean

Pavel Kishcha[a]*, Arlindo da Silva[b], Boris Starobinets[a], Charles Long[c], Olga Kalashnikova[d], and Pinhas Alpert[a]

[a]*Department of Geosciences, Tel-Aviv University, Tel-Aviv 69978, Israel;* [b]*Global Modeling and Assimilation Office, NASA/GSFC, Code 610.1, Greenbelt, MD 20771, USA;* [c]*Pacific Northwest National Laboratory, P.O. Box 999, Richland, WA, USA;* [d]*Jet Propulsion Laboratory, California Institute of Technology, Pasadena, CA 91109, USA*

(*Received 16 December 2014; accepted 20 April 2015*)

Previous studies showed that, over the global ocean, there is no noticeable hemispheric asymmetry in cloud fraction (CF). This contributes to the balance in solar radiation reaching the sea surface in the northern and southern hemispheres. In the current study, we focus on the tropical Atlantic (30° N–30° S), which is characterized by significant amounts of Saharan dust dominating other aerosol species over the North Atlantic. Our main point is that, over the tropical Atlantic, Saharan dust not only is responsible for the pronounced hemispheric aerosol asymmetry, but also contributes to significant cloud cover along the Saharan Air Layer (SAL). Over the tropical Atlantic in July, along the SAL, Moderate Resolution Imaging Spectroradiometer CF data showed significant cloud cover (up to 0.8–0.9). This significant CF along SAL together with clouds over the Atlantic Intertropical Convergence Zone contributes to the 20% hemispheric CF asymmetry. This leads to the imbalance in strong solar radiation, which reaches the sea surface between the tropical North and South Atlantic, and, consequently, affects climate formation in the tropical Atlantic. During the 10-year study period (July 2002–June 2012), NASA Aerosol Reanalysis (aka MERRAero) showed that, when the hemispheric asymmetry in dust aerosol optical thickness (AOT) was most pronounced (particularly in July), dust AOT averaged separately over the tropical North Atlantic was one order of magnitude higher than that averaged over the tropical South Atlantic. In the presence of such strong hemispheric asymmetry in dust AOT in July, CF averaged separately over the tropical North Atlantic exceeded that over the tropical South Atlantic by 20%. Both Multiangle Imaging Spectroradiometer measurements and MERRAero data were in agreement on seasonal variations in hemispheric aerosol asymmetry. Hemispheric asymmetry in total AOT over the Atlantic was most pronounced between March and July, when dust presence over the North Atlantic was maximal. In September and October, there was no noticeable hemispheric aerosol asymmetry between the tropical North and South Atlantic. During the season with no noticeable hemispheric aerosol asymmetry, we found no noticeable asymmetry in cloud cover.

1. Introduction

Hemispheric asymmetry in cloud fraction (CF) and aerosols leads to hemispheric imbalance in solar radiation reaching the surface and, consequently, affects Earth's climate. Satellite observations have been widely used in the study of aerosol optical thickness

*Corresponding author. Email: pavelk@post.tau.ac.il

(AOT) and cloud cover because of their capability to provide global coverage on a regular basis. Previous studies, using different space-borne aerosol sensors, discussed the idea that the hemispheres are asymmetric in aerosol distribution (Remer et al. 2008; Kaufman et al. 2005a; Remer and Kaufman 2006; Mishchenko and Geogdzhayev 2007; Chou, Chan, and Wang 2002; Zhang and Reid 2010; Hsu et al. 2012; Kishcha, Starobinets, and Alpert 2007, 2009). The Advanced Very High Resolution Radiometer satellite data over the ocean were used by Mishchenko and Geogdzhayev (2007) to compare monthly averaged AOT over the northern and southern hemispheres. They found a difference in AOT averaged over the two hemispheres. Chou, Chan, and Wang (2002) obtained meridional distribution of AOT over the ocean using the Sea-viewing Wide Field-of-view Sensor (SeaWiFS) satellite data for the year 1998. Hsu et al. (2012) displayed the asymmetric spatial distribution of seasonally averaged SeaWiFS AOT from 1997 to 2010. Several studies based on the Moderate Resolution Imaging Spectroradiometer (MODIS) and Multiangle Imaging Spectroradiometer (MISR) data showed that aerosol parameters are distributed asymmetrically on the two hemispheres (Remer et al. 2008; Kaufman, Boucher, et al. 2005; Remer and Kaufman 2006; Zhang and Reid 2010; Kishcha, Starobinets, and Alpert 2007, 2009). In our previous study (Kishcha et al. 2009), AOT data from three satellite sensors (MISR, MODIS-Terra, and MODIS-Aqua) were used to analyse seasonal variations of meridional AOT asymmetry over the global ocean. The asymmetry was pronounced during the April–July months, whereas there was no noticeable asymmetry during the season from September to December. Kishcha et al. (2009) mentioned that not only the northern hemisphere but also the southern hemisphere contributed to the formation of noticeable hemispheric aerosol asymmetry. During the season of pronounced hemispheric aerosol asymmetry, an increase in AOT was observed over the northern hemisphere, while a decrease in AOT was observed over the southern hemisphere. It was found that, over the global ocean, there was no noticeable asymmetry in meridional distribution of CF.

The Sahara emits dust in large quantities over the tropical Atlantic (Prospero and Lamb 2003). Previous studies have shown that desert dust particles can influence Earth's atmosphere in the following ways: directly by scattering and absorbing solar and thermal radiation, and indirectly by acting as cloud and ice condensation nuclei (Choobari, Zawar-Reza, and Sturman 2014 and references therein; Pey et al. 2013). It was shown by Wilcox, Lau, and Kim (2010) that the radiative effect of Saharan dust tends to draw the Atlantic Intertropical Convergence Zone (ITCZ) northward towards the Saharan Air Layer (SAL). Alpert et al. (1998) discussed the response of the atmospheric temperature field to the radiative forcing of Saharan dust over the North Atlantic Ocean. Dust particles over the Atlantic Ocean may essentially influence tropical cloud systems and precipitation (Kaufman, Koren, et al. 2005; Johnson, Shine, and Forster 2004; Min et al. 2009; Ben-Ami, Koren, and Altaratz 2009; Feingold et al. 2009; Rosenfeld, Rudich, and Lahav 2001).

To our knowledge, over a limited ocean area, hemispheric asymmetry of aerosols and CF relative to the equator has not been investigated to date. We chose the tropical Atlantic (30° N–30° S) because it is characterized by significant amounts of Saharan dust. We wished to determine whether the meridional CF distribution remains symmetrical relative to the equator in the presence of such strong hemispheric aerosol asymmetry. In the current study, we used the 10-year MODIS satellite data set of CF. Based on these remote-sensing data, we present evidence that Saharan dust is a causal factor of significant cloud cover along SAL, contributing to hemispheric asymmetry in cloud cover over the tropical Atlantic Ocean. This hemispheric asymmetry in cloud cover differs from that over the global ocean, where meridional CF distribution was symmetrical over the two hemispheres (Kishcha et al. 2009).

We determined and compared the contribution of desert dust and that of other aerosol species to aerosol asymmetry between the tropical North and South Atlantic oceans. Analysis of the meridional distribution of various aerosol species over the tropical Atlantic Ocean was carried out using the NASA Aerosol Reanalysis (aka MERRAero). This reanalysis was recently developed at NASA's Global Modeling Assimilation Office (GMAO) using a version of the NASA Goddard Earth Observing System-5 (GEOS-5) model radiatively coupled with Goddard Chemistry, Aerosol, Radiation, and Transport (GOCART) aerosols. An important property of GEOS-5 is data assimilation inclusion of bias-corrected AOT from the MODIS sensor on both Terra and Aqua satellites. Of course, AOT assimilation is effective only for two short periods of MODIS's appearance over the study area. All other time (18 hours per day) the GEOS-5 model works independent of MODIS (Kishcha et al. 2014).

2. GEOS-5 and the MERRA Aerosol Reanalysis (MERRAero)

GEOS-5 is the latest version of the NASA Global Modeling and Assimilation Office (GMAO) Earth system model, which was used to extend the NASA Modern Era-Retrospective Analysis for Research and Applications (MERRA) with five atmospheric aerosol components (sulphates, organic carbon, black carbon, desert dust, and sea salt). GEOS-5 includes aerosols based on a version of the GOCART model (Colarco et al. 2010; Chin et al. 2002). Both dust and sea salt have wind-speed-dependent emission functions (Colarco et al. 2010), whereas sulphate and carbonaceous species have emissions principally from fossil fuel combustion, biomass burning, and biofuel consumption, with additional biogenic sources of organic carbon. Sulphate has additional chemical production from oxidation of SO_2 and dimethylsulphide (DMS), as well as volcanic SO_2 emissions. Aerosol emissions for sulphate and carbonaceous species are based on the AeroCom version 2 hindcast inventories (http://aerocom.met.no/emissions.html). Daily biomass burning emissions are from the Quick Fire Emission Dataset (QFED) and are derived from MODIS fire radiative power retrievals (Darmenov and da Silva 2013). GEOS-5 also includes an assimilation of AOT observations from the MODIS sensor on both Terra and Aqua satellites. The obtained 10-year (July 2002–June 2012) MERRA-driven aerosol reanalysis (MERRAero) data set was applied to the analysis of hemispheric aerosol asymmetry in the current study. To verify the obtained meridional aerosol distribution based on MERRAero, we used the MISR monthly global 0.5° × 0.5° AOT data set available over the study period.

3. Method

Over the tropical Atlantic Ocean (30° N–30° S), variations of zonal-averaged AOT as a function of latitude were used to analyse meridional aerosol distribution, following our previous study (Kishcha et al. 2009). This included total AOT and AOT of various aerosol species. In Table 1, X stands for the average AOT over some specified area in the tropical Atlantic; X_N is the average AOT over the tropical North Atlantic; and X_S is the average AOT over the tropical South Atlantic. To quantify hemispheric AOT asymmetry, the hemispheric ratio (R) of X_N to X_S was estimated. The hemispheric ratio is equal to 1 in the case of the two parts of the tropical Atlantic holding approximately the same averaged AOT, whereas the ratio is greater (less) than 1 if the North (South) Atlantic dominates the other one. Standard deviation of the reported hemispheric ratio (Table 1) was estimated in accordance with the following formula by Ku (1966) and NIST/SEMATECH (2006):

$$C_R = \frac{1}{\sqrt{N}} \frac{X_N}{X_S} \sqrt{\frac{{C_N}^2}{{X_N}^2} + \frac{{C_S}^2}{{X_S}^2} - 2\frac{{C_{N,S}}^2}{X_N X_S}}, \quad (1)$$

where C_N and C_S are standard deviations of zonal-averaged AOTs in the tropical North and South Atlantic oceans, respectively, C_{NS} is their covariance, and $N = 120$ stands for the number of months in the MISR/MERRAero AOT monthly data set used.

Table 1. Average AOT and CF over the tropical North (X_N) and South (X_S) Atlantic and their hemispheric ratio (R)[a]. Ten-year MERRAero AOT, MISR AOT, and MODIS CF data were used.

Data set	$X_N \pm \sigma_N$	$X_S \pm \sigma_S$	$R \pm \sigma_R$
MISR AOT	0.25 ± 0.06	0.15 ± 0.05	1.70 ± 0.06
MERRAero AOT	0.19 ± 0.05	0.12 ± 0.05	1.61 ± 0.06
MODIS CF	0.66 ± 0.09	0.61 ± 0.06	1.08 ± 0.01

Note: [a]Standard deviations of X_N, X_S, and R are designated by σ_N, σ_S, and σ_R, respectively.

Variations of meridional aerosol distributions were analysed using Version 3.1 of MISR Level 3 AOT measurements and MERRAero data during the 10-year period, from July 2002 to June 2012. The MISR swath width is about 380 km and global coverage is obtained every nine days. MISR AOT has been extensively validated against Aerosol Robotic Network (AERONET) Sun photometer measurements over different regions (Matronchik et al. 2004; Christopher and Wang 2004; Kalashnikova and Kahn 2008; Liu et al. 2004). For the purpose of comparing meridional distributions of cloud cover with those of AOT during the same 10-year period (July 2002–June 2012), Collection 5.1 of MODIS–Terra Level 3 monthly daytime CF data, with horizontal resolution of 1° × 1°, was used (Ackerman et al. 1998; Frey et al. 2008; King et al. 2003). In Table 1, for CF, the definition of X, X_N, and X_S are similar to those for AOT. Furthermore, to analyse meridional rainfall distribution, the Tropical Rainfall Measuring Mission (TRMM) monthly 0.25° × 0.25° Rainfall Data Product (3B43 Version 7) was used (Huffman et al. 2007). MODIS CF data and TRMM data were acquired using the GES-DISC Interactive Online Visualization and Analysis Infrastructure (Giovanni) as part of NASA Goddard Earth Sciences (GES) Data and Information Services Center (DISC) (Acker and Leptoukh 2007).

4. Results

4.1. Ocean zone with the predominance of desert dust aerosols

MERRAero showed that the Sahara emits a significant amount of dust into the atmosphere over the Atlantic Ocean (Figure 1(*a*), (*c*), and (*e*)). With respect to different oceans, MERRAero showed that desert dust dominates all other aerosol species only over the Atlantic Ocean. Figure 1(*b*), (*d*), and (*f*) represents spatial distribution of the ratio of dust AOT to AOT of all other aerosol species. The red contour lines represent the boundary of the zone where dust AOT is equal to AOT of all other aerosol species. One can see that, throughout the 10-year period under consideration, over the Atlantic Ocean within the latitudinal zone between 7° N and 30° N, Saharan dust dominates other aerosol species

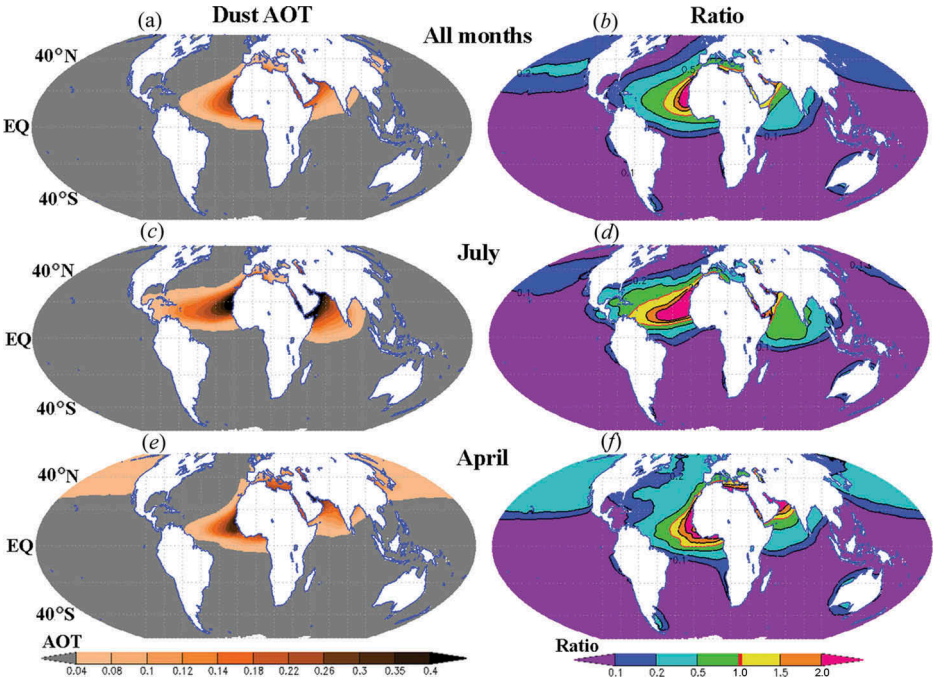

Figure 1. Spatial distributions of ((*a*), (*c*), and (*e*)) dust AOT (DU) and ((*b*), (*d*), and (*f*)) the ratio of DU to AOT of all other aerosol species, based on the 10-year MERRAero data. In the right panel, the red contour line represents the boundary of the zone where dust AOT is equal to AOT of all other aerosol species.

(Figure 1(*b*)). The longitudinal dimension of this zone is subject to seasonal variability. During the dusty season from March to July, the zone of dust predominance occupies a significant part of the tropical Atlantic between North Africa and Central America. Specifically, as shown in Figure 1(*d*), in July, the zone of dust predominance is extremely extensive. By contrast, from October to February, this zone is observed only over some limited territory close to North Africa.

Desert dust can be seen not only over the Atlantic Ocean, but also over the Pacific and Indian oceans (Figure 1(*a*), (*c*), and (*e*)). However, outside of the Atlantic Ocean, one can see only limited zones of desert dust predominance over the Mediterranean Sea and over the Arabian Sea (Figure 1(*b*), (*d*), and (*f*)). Therefore, the tropical North Atlantic Ocean is the largest ocean area where dust particles determine the atmospheric aerosol content, based on MERRAero data.

4.2. *Meridional distribution of total AOT over the tropical Atlantic Ocean*

Figure 2(*a*) represents meridional distribution of 10-year mean AOT (July 2002–June 2012) zonal-averaged over the tropical Atlantic Ocean. MERRAero was found to be similar to the meridional AOT distribution, based on the MISR data (Figure 2(*a*)). Specifically, MERRAero was able to reproduce the hemispheric asymmetry in the AOT distribution, including a monomodal maximum in the tropical North Atlantic and a minimum in the tropical South Atlantic. This monomodal AOT maximum was discussed in our previous study (Kishcha et al. 2009). Both MISR and MERRAero showed that, in

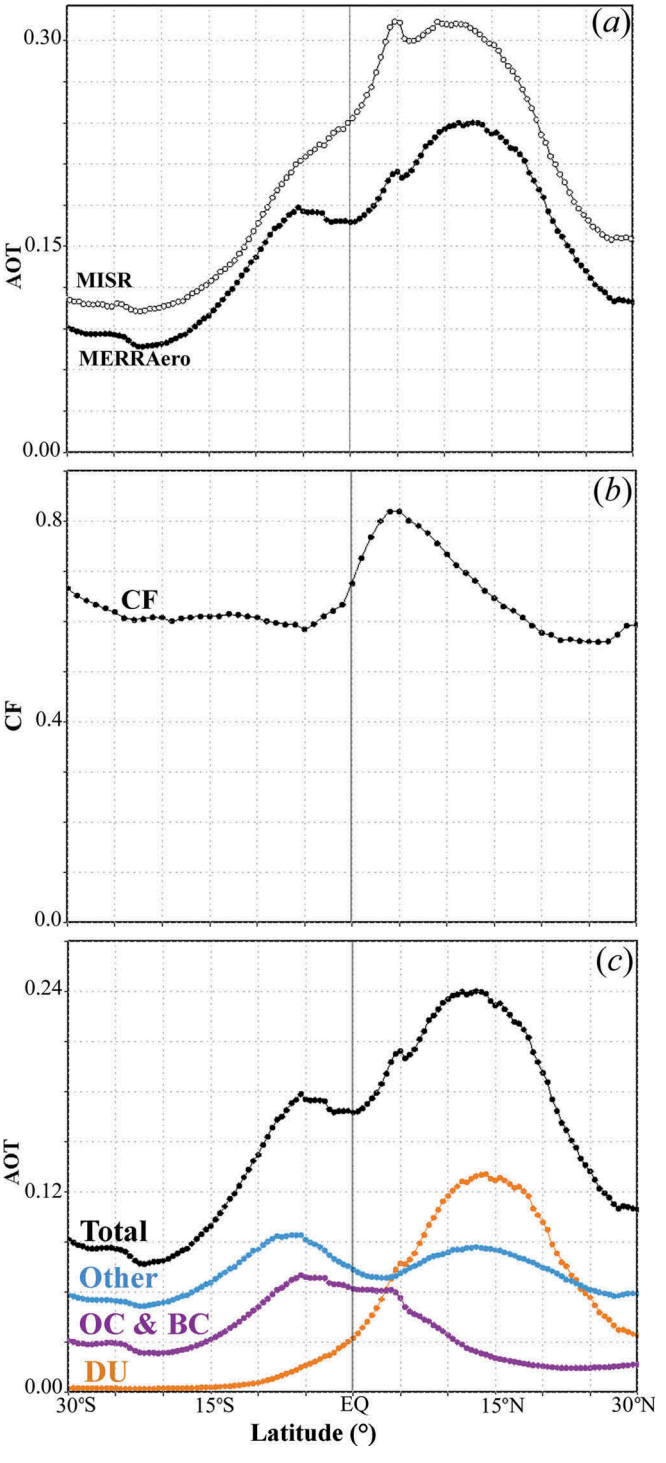

Figure 2. The meridional distribution of 10-year mean AOT/CF zonal-averaged over the Atlantic Ocean (60° W–0° E): (a) total AOT based on MERRAero and MISR data; (b) MODIS CF; (c) MERRAero total AOT, dust AOT (DU), organic and black carbon AOT (OC & BC), and other aerosol species AOT (Other). The vertical lines designate the position of the equator.

the minimum, the AOT values were three times lower than those in the maximum. We quantified meridional AOT asymmetry relative to the equator in the tropical Atlantic Ocean (30° N–30° S) by obtaining the hemispheric ratio (R_{AOT}) of AOT averaged separately over the tropical North Atlantic to AOT averaged over the tropical South Atlantic: R_{AOT} was estimated to be about 1.7 (Table 1). This means that, over the 10-year period under consideration, there were many more aerosol particles over the tropical North Atlantic than over the tropical South Atlantic.

4.3. *Seasonal variations of meridional distribution of AOT*

For each month of the year, we analysed variations of meridional distribution of AOT over the tropical Atlantic Ocean (Figure 3). It was found that the meridional AOT distribution

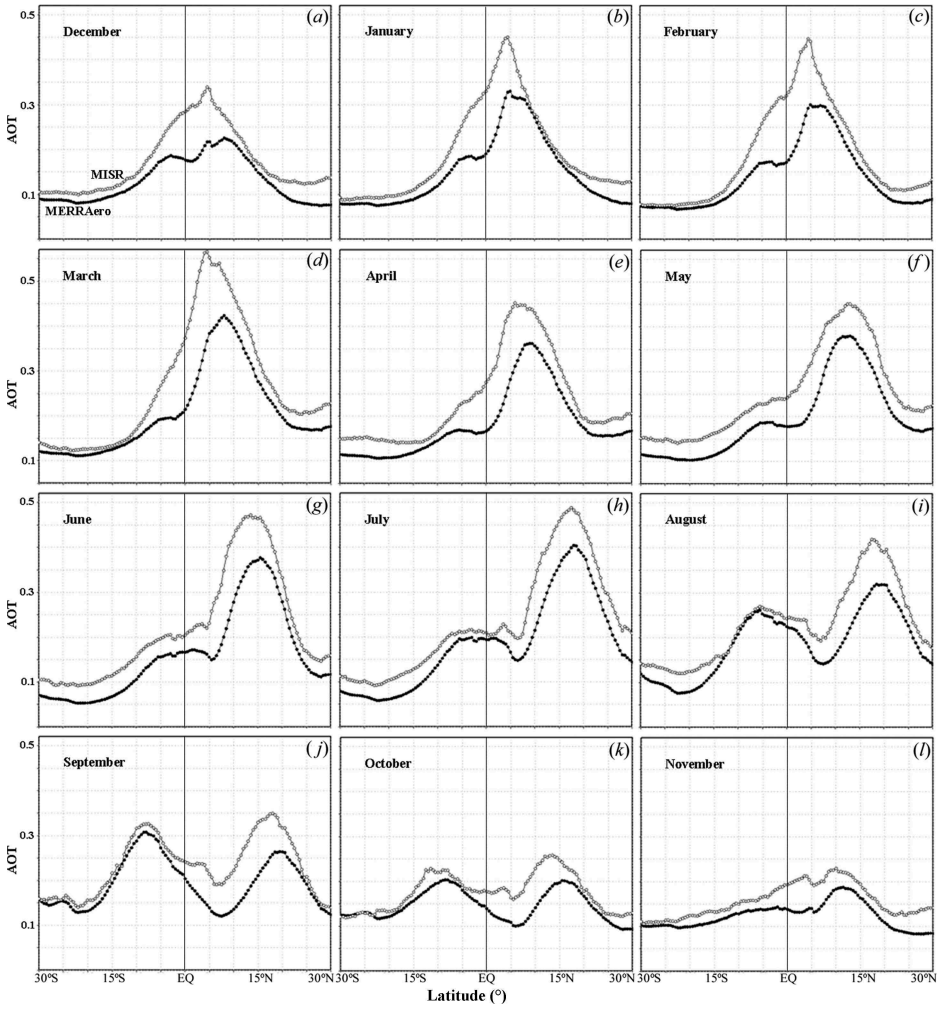

Figure 3. Meridional distribution of MISR and MERRAero total AOT, zonal-averaged over the Atlantic Ocean, for all months of the year. The vertical lines designate the position of the equator.

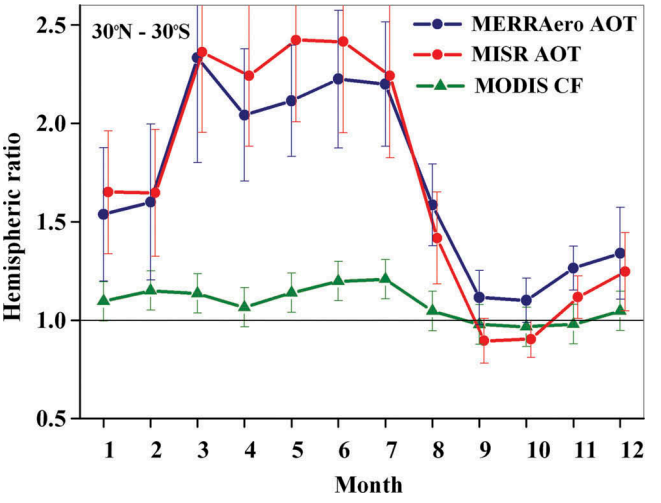

Figure 4. Month-to-month variations of the hemispheric ratio (R) of MISR AOT, MERRAero AOT, and MODIS cloud fraction (CF) over the tropical Atlantic Ocean (30° N–30° S). The error bars show the standard deviation of R.

is seasonal dependent. In particular, both MISR and MERRAero were in agreement that the monomodal AOT maximum, a characteristic feature of hemispheric asymmetry in AOT, exists but not in each month. In the months from September to October, two AOT maxima can be observed: one maximum in the North Atlantic and another one in the South Atlantic.

Figure 4 represents month-to-month variations of the hemispheric ratio R_{AOT} over the tropical Atlantic for each month of the year. Both MISR and MERRAero showed that meridional AOT asymmetry was most pronounced during the season from March to July (Figure 4). One can see that, from month to month during the year, R_{AOT} ranges from 1 to 2.4, while during the season of pronounced hemispheric aerosol asymmetry (March–July) R_{AOT} ranges from 2.0 to 2.4. In September and October, R_{AOT} was close to 1, indicating no noticeable asymmetry (Figure 4).

4.4. *Meridional distribution of AOT of various aerosol species*

Figure 2(*c*) represents meridional distribution of 10-year mean MERRAero AOT for total AOT (Total), dust AOT (DU), organic and black carbon aerosol AOT (OC & BC), and AOT of other aerosol species (Other), zonal-averaged over the tropical Atlantic Ocean. One can see that meridional dust distribution is much more asymmetric relative to the equator than meridional distribution of OC & BC and other aerosol species. The hemispheric asymmetry of DU, characterized by the hemispheric ratio (R_{DU}) of dust AOT, was about 11 (Table 2). Such strong asymmetry in meridional distribution of desert dust over the ocean can be explained by its transport by winds from the Sahara to the ocean in the North Atlantic. Being the major contributor to the AOT maximum in the North Atlantic, Saharan dust was responsible for the pronounced meridional AOT asymmetry in total AOT over the tropical Atlantic Ocean. Carbon aerosols also displayed some hemispheric asymmetry characterized by the hemispheric ratio $R_{OC\&BC} = 0.7$, although this asymmetry

Table 2. The hemispheric ratio (±standard deviation) of dust AOT (DU), organic and black carbon AOT (OC & BC), other aerosol species AOT (Other), and MODIS CF over the tropical Atlantic Ocean (30° N–30° S). Ten-year MERRAero data and MODIS CF data were used.

Month	DU	OC & BC	Other	MODIS CF
All months	11.50 ± 1.20	0.70 ± 0.10	1.10 ± 0.10	1.08 ± 0.01
January	6.10 ± 2.30	1.30 ± 0.50	1.10 ± 0.10	1.10 ± 0.07
February	4.20 ± 1.80	1.20 ± 0.40	1.20 ± 0.10	1.15 ± 0.09
March	6.90 ± 3.20	2.00 ± 0.40	1.20 ± 0.10	1.14 ± 0.10
April	8.80 ± 4.10	2.70 ± 0.40	1.20 ± 0.10	1.07 ± 0.09
May	21.00 ± 10.10	1.70 ± 0.30	1.20 ± 0.10	1.14 ± 0.07
June	23.50 ± 10.80	0.90 ± 0.30	1.30 ± 0.10	1.20 ± 0.09
July	29.30 ± 10.30	0.70 ± 0.30	1.30 ± 0.20	1.21 ± 0.08
August	25.00 ± 8.50	0.40 ± 0.10	1.10 ± 0.10	1.04 ± 0.07
September	23.80 ± 6.70	0.20 ± 0.10	0.90 ± 0.10	0.98 ± 0.05
October	17.00 ± 4.30	0.20 ± 0.10	0.80 ± 0.10	0.97 ± 0.05
November	9.70 ± 2.30	0.70 ± 0.20	0.80 ± 0.10	0.98 ± 0.05
December	6.80 ± 1.90	1.00 ± 0.30	0.90 ± 0.10	1.05 ± 0.05

was much less pronounced than that of desert dust (Figure 2(*c*) and Table 2). Meridional distribution of AOT of other aerosol species was almost symmetrical (R_{Other} is 1.1) (Table 2). Therefore, aerosols over the tropical Atlantic can be divided into two groups with different meridional distributions relative to the equator: dust and carbonaceous aerosols were distributed asymmetrically, whereas other aerosol species were distributed more symmetrically.

MERRAero showed that seasonal variations of transatlantic Saharan dust transport determined the seasonal variations of meridional dust asymmetry. During May–July, when hemispheric asymmetry in dust AOT over the tropical North Atlantic was most pronounced, dust AOT averaged separately over the tropical North Atlantic was one order of magnitude higher than that averaged over the tropical South Atlantic (Table 2). In July, the most pronounced hemispheric asymmetry of dust AOT was characterized by the hemispheric ratio R_{DU} of about 30 (Table 2).

When dust presence over the North Atlantic was minimal, the contribution of other aerosol species to the meridional distribution of total AOT could be significant. In particular, in December, the maximum in OC & BC at low latitudes (due to the transport of biomass burning smoke) contributed significantly to the maximum in total AOT in the tropical North Atlantic (Figure 5(*a*)). Note that the reason for the aforementioned transport of biomass burning aerosols is the burning of agricultural waste in the Sahelian region of northern Africa. This burning activity is maximal during December–February (Haywood et al. 2008). MERRAero showed that no noticeable hemispheric asymmetry of total AOT was observed during September and October (Figure 4). This is because the contribution of carbonaceous aerosols (OC & BC) to total AOT over the South Atlantic is approximately equal to the contribution of Saharan dust to total AOT in the North Atlantic (Figure 5). The reason for the observed increase in OC & BC over the South Atlantic in September and October is that these months fall within the burning period in Central Africa, where slash-and-burn agriculture is prevalent (Tereszchuk et al. 2011). In September and October, AOT of carbonaceous aerosols over the tropical South

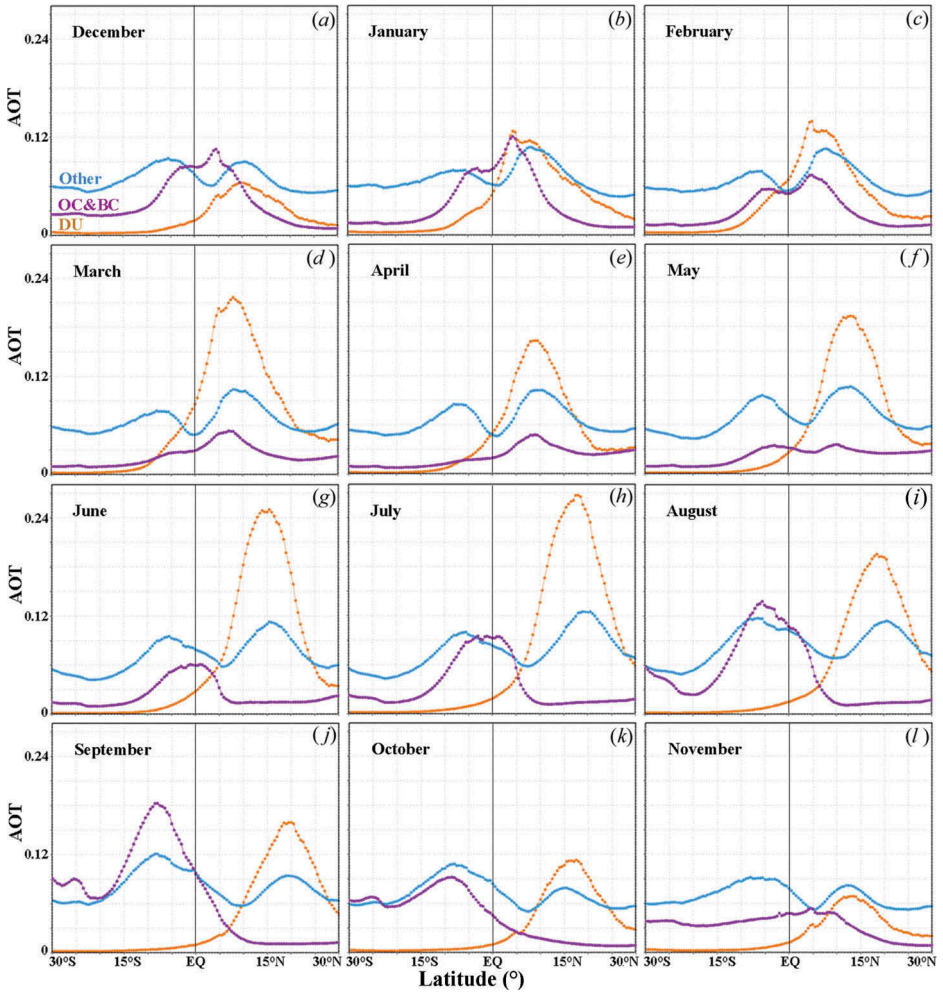

Figure 5. Meridional distribution of dust AOT (DU), organic and black carbon aerosol AOT (OC & BC), and other aerosol species AOT (Other), zonal-averaged over the Atlantic Ocean, for all months of the year, based on 10-year MERRAero data. The vertical lines designate the position of the equator.

Atlantic was five times higher than that over the tropical North Atlantic ($R_{OC\&BC} = 0.2$) (Table 2).

Meridional distribution of AOT of other aerosol species remains more symmetrical than dust and carbonaceous aerosols throughout all months (the hemispheric ratio R_{Other} ranged from 0.8 to 1.3) (Table 2). This group includes marine aerosols, such as sea salt and DMS aerosols, which are produced everywhere in the tropical Atlantic Ocean (Lewis and Schwartz 2004; O'Dowd and de Leeuw 2007).

4.5. *Meridional distribution of CF*

We analysed the meridional distribution of cloud cover over the tropical (30° N–30° S) Atlantic Ocean, which includes the area of transatlantic Saharan dust transport within

SAL. Figure 2(*b*) represents the meridional distribution of 10-year mean CF, zonal-averaged over the Atlantic Ocean. One can see the local maximum near the equator due to clouds concentrated over the Intertropical Convergence Zone: this maximum shifts to the north from the equator. Despite this CF maximum, the hemispheric CF ratio (R_{CF}), characterized by the ratio of CF averaged separately over the tropical North and over the South Atlantic did not exceed 1.1 (Table 1).

As mentioned in Section 4.4, MERRAero showed that dust and carbonaceous aerosols were distributed asymmetrically in relation to the equator, whereas other aerosol species were distributed more symmetrically. During the period of pronounced meridional AOT asymmetry over the tropical Atlantic from May to July, dust AOT averaged separately over the tropical North Atlantic was about one order of magnitude higher than that averaged over the tropical South Atlantic (Table 2). In July, the hemispheric ratio R_{DU} was roughly 30. In the presence of such strong meridional dust asymmetry, in July, R_{CF} reached 1.2 (Table 2 and Figure 4). As shown in a previous study (Kishcha et al. 2009), over the global ocean, R_{AOT} was about 1.5, whereas R_{CF} was 1. Therefore, in contrast to the global ocean (where meridional CF distribution was symmetrical over the two hemispheres), over the tropical Atlantic in July, CF averaged separately over the tropical North Atlantic exceeded CF averaged over the tropical South Atlantic by 20%. In September–October, when there was no hemispheric asymmetry in total AOT over the tropical Atlantic (R_{AOT} was close to 1), meridional CF distribution was also almost symmetrical (R_{CF} was equal to 1, (Table 2 and Figure 4)).

Figure 6 represents the meridional distribution of MODIS CF and TRMM-accumulated rainfall, zonal-averaged over the tropical Atlantic Ocean, for all months of the year. One can see some changes in CF from month to month on the high background level of approximately 0.6. This background level of CF is almost the same over the tropical North and South Atlantic oceans.

In each month, the main CF maximum coincides with the Atlantic Ocean Intertropical Convergence Zone, which is characterized by intensive rainfall (Figure 6). In the summer months (when pronounced meridional dust asymmetry was observed), MODIS CF data showed significant CF to the north from the main CF maximum, over the latitudes of transatlantic dust transport within the SAL (Figure 6 (*g*)–(*i*)). Saharan dust travels across the Atlantic Ocean within the hot and dry SAL (Dunion and Velden 2004). The SAL's base is at ~900–1800 m and the top is usually below 5500 m (Diaz, Carlson, and Prospero 1976). The significant CF along SAL, together with the Atlantic ITCZ (centred over the tropical North Atlantic), contributed to the above-mentioned hemispheric CF asymmetry. Following is our analysis of CF in the area of the SAL in July, when the most pronounced meridional dust asymmetry was observed.

4.5.1. CF in the area of the SAL in July

Figure 7 represents the meridional distribution of the 10-year mean of MERRAero dust AOT, MODIS-Terra CF, and TRMM-accumulated rainfall, zonal-averaged over the Atlantic Ocean (60° W–0° E). The near-equatorial maximum in the meridional distribution of TRMM-accumulated rainfall indicates the position of the North Atlantic Ocean ITCZ (Figure 7). One can see that, in July, when dust presence over the Atlantic is maximal, the meridional distribution of CF becomes essentially asymmetric with respect to the centre of ITCZ. In particular, significant CF up to 0.8 is seen to the

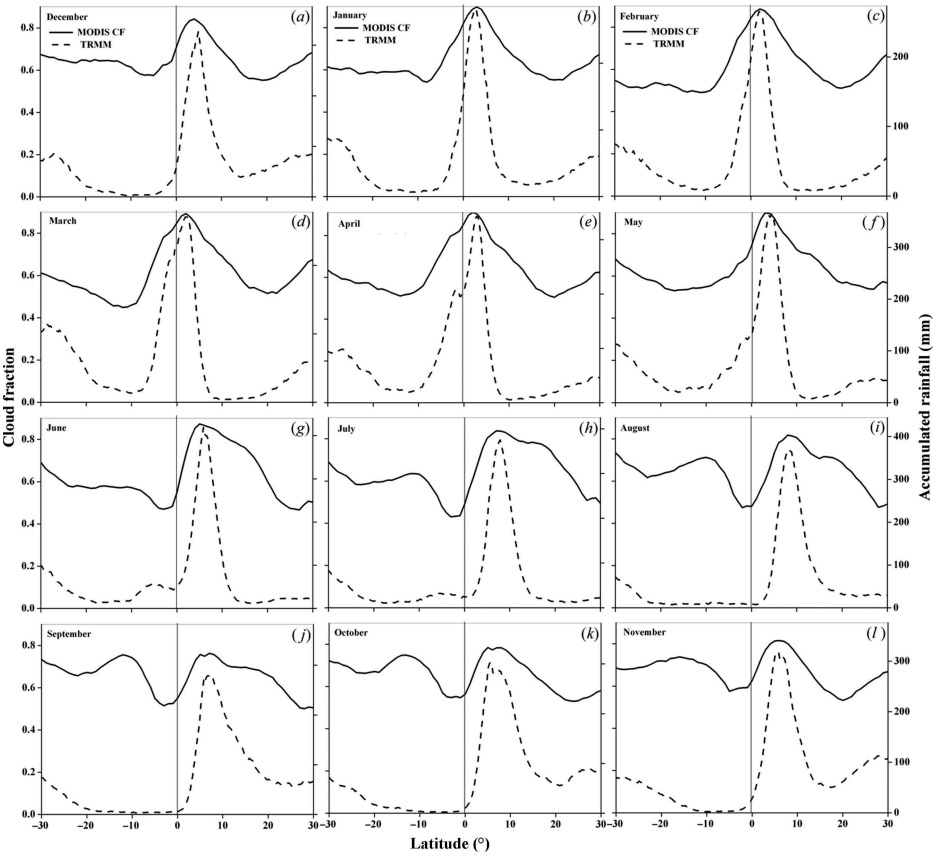

Figure 6. Meridional distribution of MODIS–Terra CF and TRMM-accumulated rainfall, zonal-averaged over the tropical Atlantic Ocean, for all months of the year. The vertical lines designate the position of the equator.

north of ITCZ, over the latitudes with SAL presence (12° N–24° N) (Figure 7). These values are higher than the 10-year mean MODIS CF over the tropical North Atlantic (0.66) (Table 1). One can consider that, in the North Atlantic, the wide maximum in the meridional distribution of CF consists of two different partly overlapping maxima: one CF maximum located within ITCZ and the other CF maximum located to the north of ITCZ, over the ocean area where Saharan dust is transported within the SAL across the Atlantic (Figure 7).

More detailed information about the aforementioned two partly overlapping maxima in the meridional distribution of CF in July can be obtained from a comparison between the spatial distribution of 10-year mean MERRAero dust AOT and MODIS CF over the tropical North Atlantic (Figure 8(*a*) and (*b*)). It is clearly seen that the ocean area with Saharan dust transported across the Atlantic is covered by cloudiness characterized by significant values of MODIS CF up to 0.8–0.9. This CF is higher than the 10-year mean MODIS CF over the tropical North Atlantic (0.66) (Table 1). Note that there is a strong difference between the two zones of significant CF in the North Atlantic. High values of CF within ITCZ are accompanied by intensive rainfall (Figure 8(*b*) and (*c*)). In contrast, the area of SAL with significant CF (12° N–24° N) is characterized

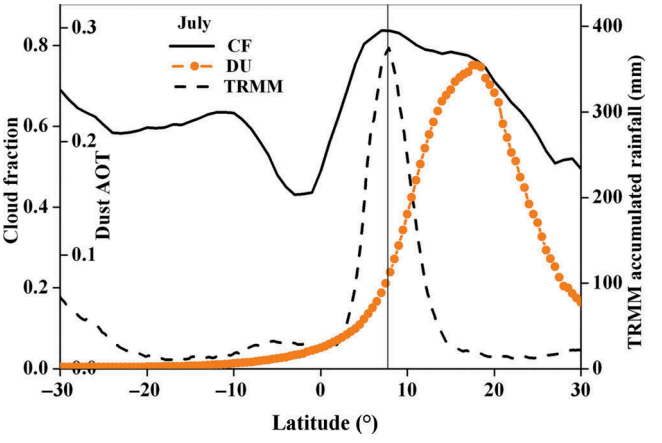

Figure 7. Meridional distribution of 10-year mean MODIS–Terra cloud fraction (CF), TRMM-accumulated rainfall, and MERRAero dust AOT (DU), zonal-averaged over the Atlantic Ocean (60° W–0° E), in July. The near-equatorial maximum in meridional distribution of TRMM-accumulated rainfall indicates the position of the North Atlantic Ocean Intertropical Convergence Zone (ITCZ). The vertical line designates the position of the centre of ITCZ.

by essentially lower precipitation (Figure 8(*b*) and (*c*)). The spatial distribution of 10-year mean monthly accumulated rainfall over the North Atlantic in July (Figure 8(*c*)) was obtained using the TRMM monthly rainfall data product (3B43 Version 7) (Huffman et al. 2007).

To quantify changes in dust AOT, MODIS-based CF, and TRMM monthly accumulated rainfall with distance from the Sahara, we analysed the 10-year mean (July 2002–June 2012) of these parameters over six zones, each 6° × 6°, located along the SAL, in accordance with the direction of dust transport (Figure 8(*a*)). In July, there was a decrease of approximately 300% in dust AOT from zone 1 to zone 6 (Figure 9(*a*)). The reason for the decrease in dust AOT with increasing distance from dust sources in the Sahara is gravitational settling of dust particles (mainly coarse fraction). As shown in Figure 9(*a*) and (*b*), the strong decrease in dust AOT from zone 1 to zone 3 was not accompanied by any changes in TRMM-accumulated rainfall. Therefore, the washing out of aerosols by rainfall does not account for the aerosol spatial decrease with distance from the Sahara. Consequently, it proves that gravitational settling of dust particles accounts for the aerosol spatial decrease with distance from the Sahara.

MODIS CF also decreased from zone 1 to zone 3, although less pronounced than dust (Figure 9(*b*)). Over zones 1–3, there was significant CF in the presence of limited precipitation less than 20 mm month^{-1}. This indicates that clouds in zones 1–3 were not developed enough to produce intensive precipitation. This can be explained by the effect of temperature inversion below the SAL base on cloud formation (Prospero and Carlson 1972; Kaufman, Koren, et al. 2005).

To examine temperature inversion over the specified zones, we analysed the vertical profiles of 10-year mean MERRA Reanalysis atmospheric temperature in July, averaged over the specified zones. As shown in Figure 10, the temperature inversion existed over zones 1–4 and it disappeared over zones 5 and 6. The observed temperature inversion over zones 1–4 (Figure 10) prevented deep cloud formation, which explains the observed limited precipitation in these zones (Figure 9(*b*)). In the absence of temperature inversion

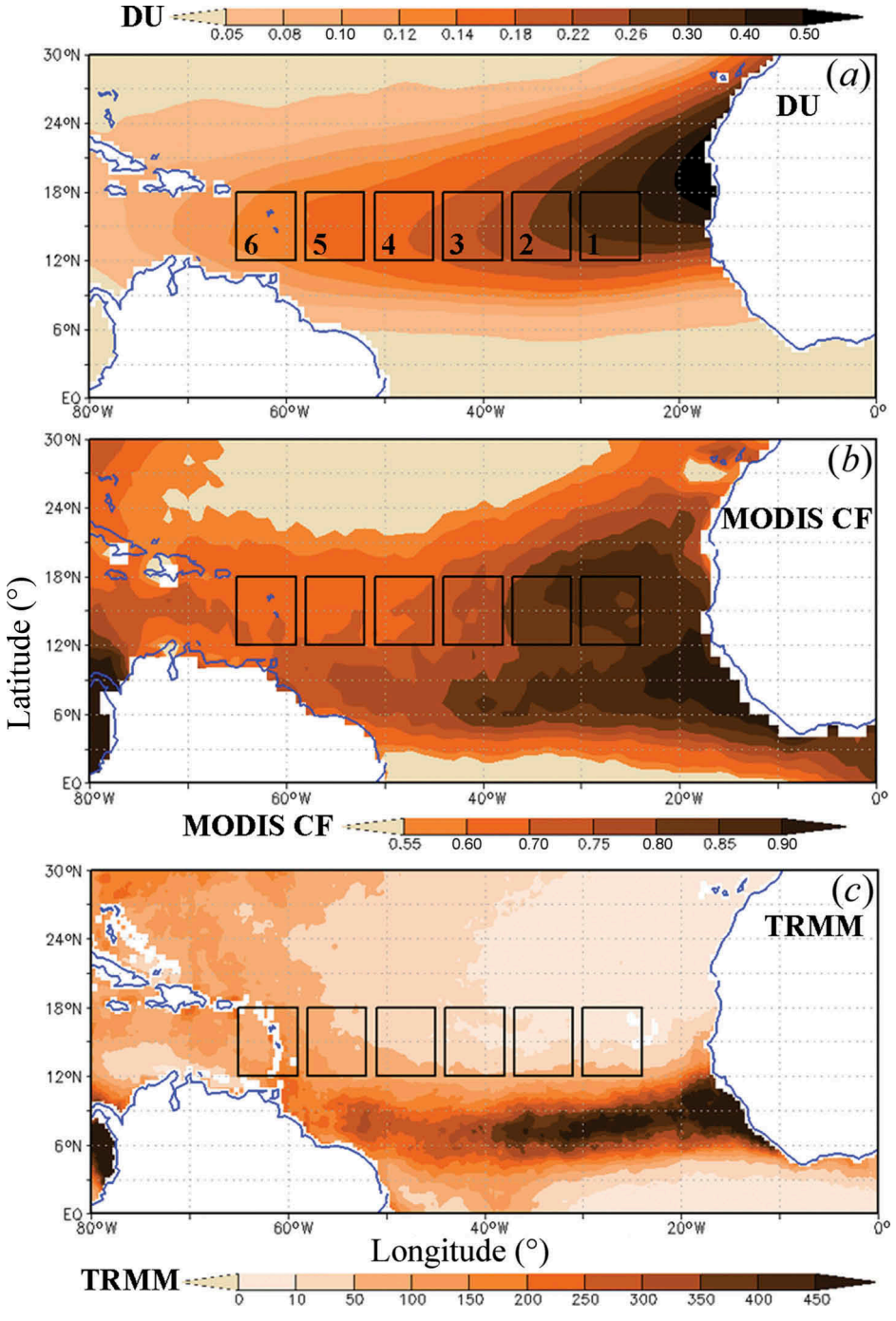

Figure 8. Spatial distributions of 10-year mean (*a*) MERRAero dust AOT (DU), (*b*) MODIS–Terra CF, and (*c*) TRMM-accumulated rainfall over the North Atlantic in July. The geographic coordinates of the specified zones are as follows: zone 1 (12° N–18° N; 30° W–24° W), zone 2 (12° N–18° N; 37° W–31° W), zone 3 (12° N–18° N; 44° W–38° W), zone 4 (12° N–18° N; 51° W–45° W), zone 5 (12° N–18° N; 58° W–52° W), zone 6 (12° N–18° N; 65° W–59° W).

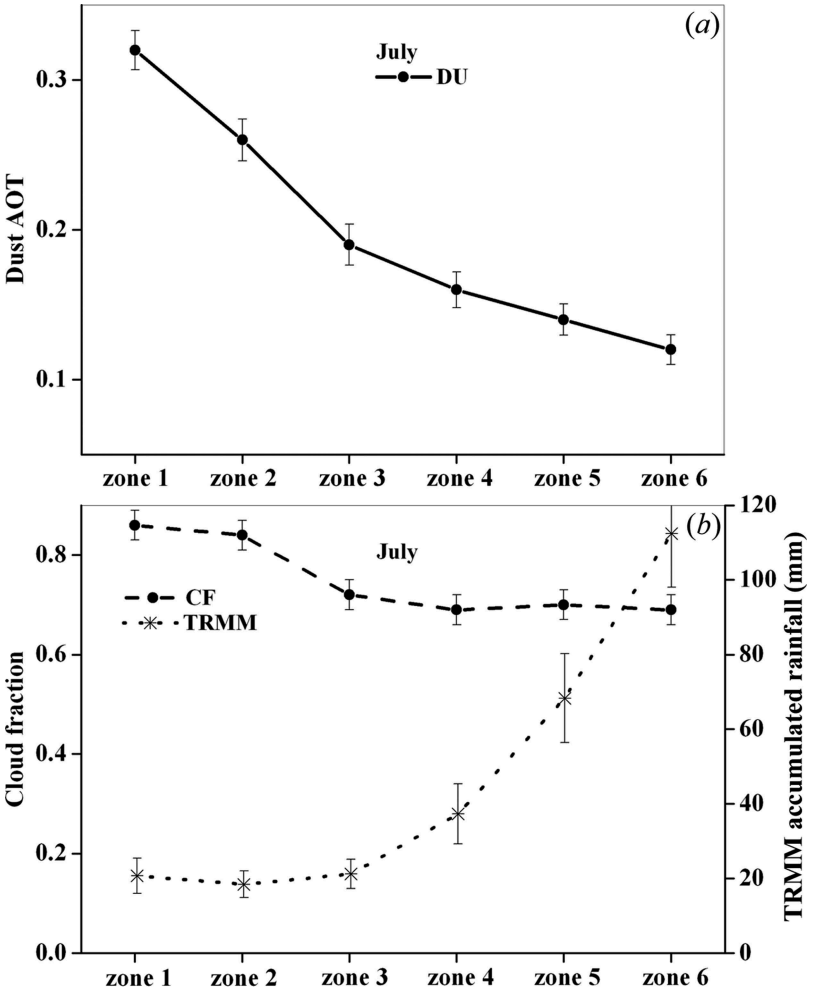

Figure 9. Zone-to-zone variations of (*a*) MERRAero dust AOT (DU); (*b*) MODIS–Terra CF and TRMM-accumulated rainfall over the specified zones in July, averaged over the 10-year study period (2002–2012). The error bars show the standard error of mean.

over zones 5 and 6 (Figure 10), one can consider the presence of developed cumulus clouds, which were capable of producing intensive rainfall. Such developed cumulus clouds could explain the observed precipitation up to 110 mm month^{-1} over zones 5 and 6 (Figure 9(*b*)).

4.5.2. *Influence of dust loading on CF in the area of SAL*

As mentioned, the observed temperature inversion over zones 1–4 prevents deep cloud formation. On the other hand, meteorological conditions below the temperature inversion at the SAL base include significant atmospheric humidity and the presence of large amounts of settling dust particles together with marine aerosols.

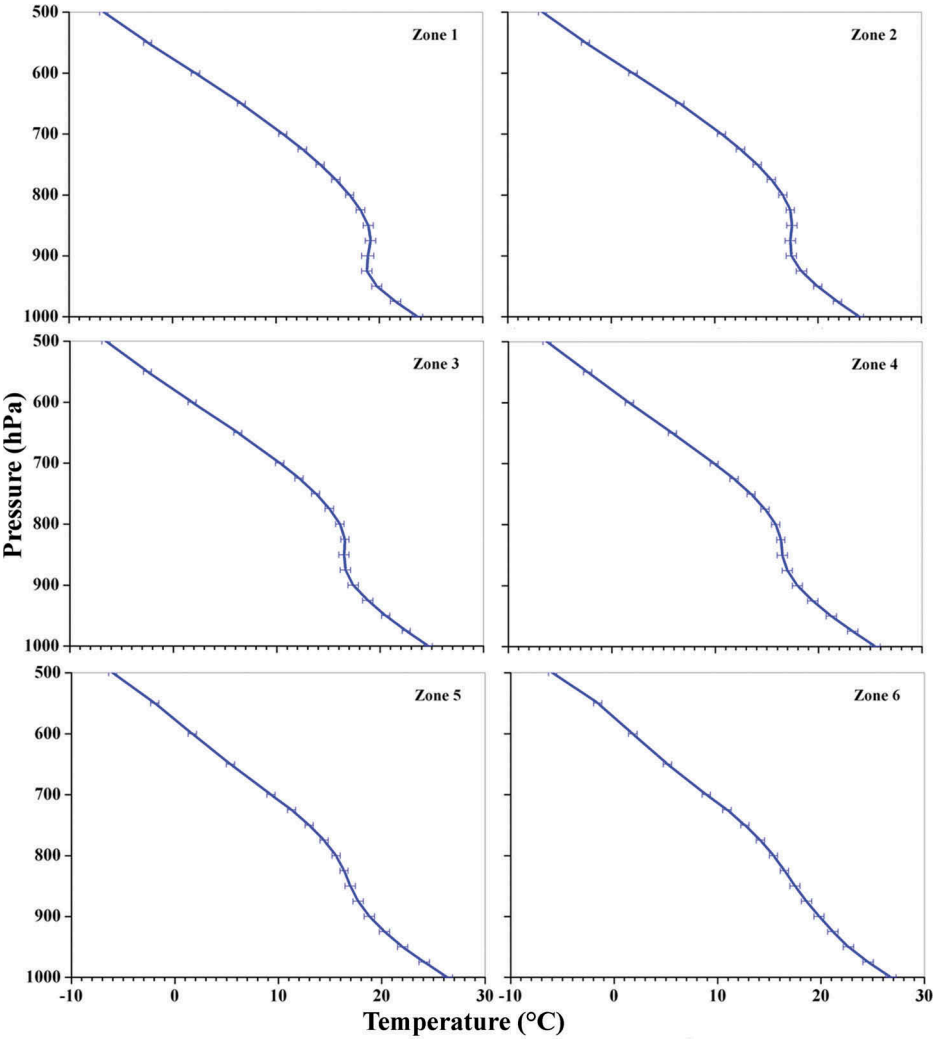

Figure 10. Vertical profiles of 10-year mean MERRA Reanalysis atmospheric temperature (°C) in July, averaged over the specified zones along the route of transatlantic dust transport. The error bars show the standard deviation of temperature.

As is known, aerosol species often combine to form mixed particles, with properties different from those of their components (Andreae, Hegg, and Baltensperger 2009). Mineral dust particles are known to be not very efficient cloud condensation nuclei (CCN), unless they are coated with soluble materials (Andreae, Hegg, and Baltensperger 2009). Using aeroplane measurements, Levin et al. (2005) showed that dust transport over the sea could lead to sea-salt coating on dust particles. Coating settling dust particles with sea salt could modify them into efficient CCN. Being below the temperature inversion and acting as efficient CCN, Saharan dust particles coated with soluble material contribute to the formation of shallow stratocumulus clouds. This physical mechanism, based on the indirect effect of Saharan dust on stratocumulus clouds below the temperature inversion, could explain the observed

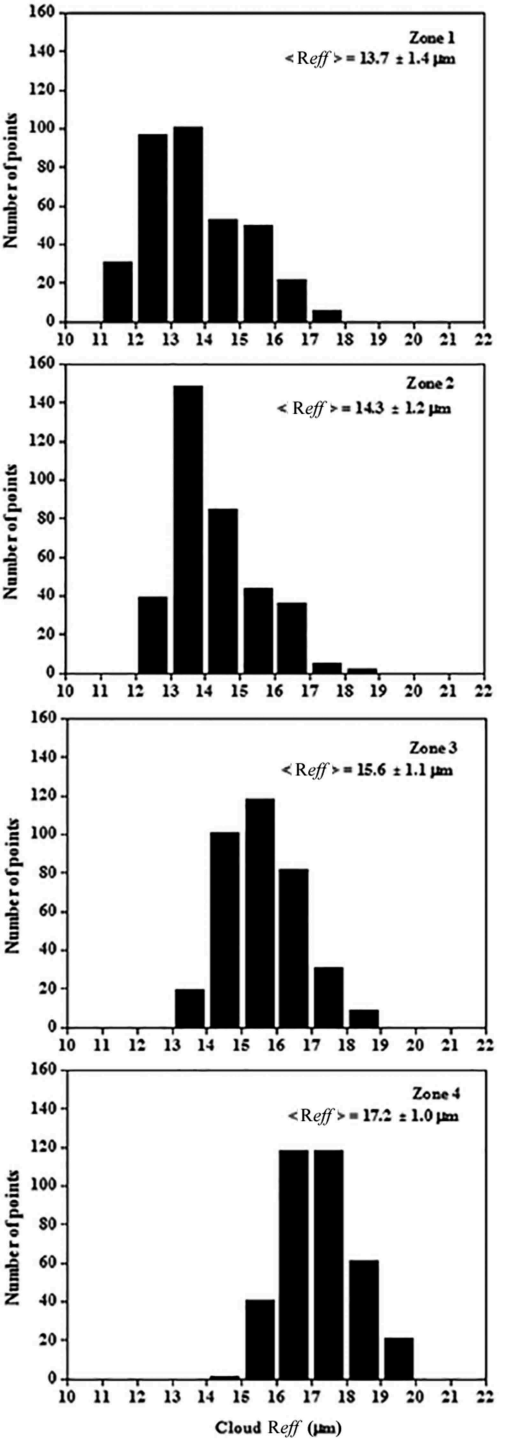

Figure 11. The histograms of the effective radius (R_{eff}) of cloud droplets for liquid water clouds in the specified zones 1–4 along SAL, based on MODIS Level 3 gridded monthly data with resolution 1° × 1° during the 10-year study period in July. The average R_{eff} (±its standard deviation) in each zone is shown.

significant cloud cover (CF up to 0.8–0.9) along the SAL. The significant CF along SAL contributes to hemispheric CF asymmetry over the tropical Atlantic. This leads to hemispheric imbalance in strong solar radiation reaching the sea surface in the tropical Atlantic Ocean.

To examine the properties of clouds in the area of SAL, we analysed available data on the effective radius of cloud droplets. Figure 11 represents histograms of the effective radius (R_{eff}) of cloud droplets for liquid water clouds in the specified zones 1–4 along SAL, based on MODIS L3 gridded monthly data (1° × 1°) during the 10-year study period in July. The data were supplied by the Giovanni database. It is obvious that the cloud droplet effective radius increases from zone 1 to zone 4 (Figure 11). One can see a systematic shift in the whole histogram to higher values of R_{eff} from zone 1 to zone 4. This can be explained by the decrease in CCN numbers associated with the decreasing numbers of settling Saharan dust particles with distance from the Sahara, in accordance with the decrease in dust AOT shown in Figure 9(*a*).

Thus, the cloud droplet effective radius in zone 4 was larger than in zones 1–3. This could lead to some increase in precipitation in zone 4. Indeed, as shown in Figure 9(*b*), TRMM-accumulated rainfall in zone 4 was more intensive than over zones 1–3. This supports the above-mentioned physical mechanism of cloud formation below the temperature inversion at the SAL base.

In accordance with the above-mentioned mechanism of cloud formation along SAL, there are different cloud types over zones 1–4 on the one hand and over zones 5–6 on the other hand. Over zones 1–4, we consider the presence of shallow stratocumulus clouds below the temperature inversion at the SAL base. These shallow stratocumulus clouds are characterized by limited precipitation. Over zones 5–6, we consider the presence of developed cumulus clouds capable of producing strong precipitation up to 110 mm month^{-1}.

4.5.3. *Possible MODIS CF contamination by heavy dust loading*

Collection 5 of MODIS–Terra monthly daytime CF data used in the current study are derived from the standard cloud mask product based on the cloud mask algorithm MOD35 (Ackerman et al. 1998; Frey et al. 2008). In heavy dust loading situations, such as dust storms over deserts, MOD35 may flag the aerosol-laden atmosphere as cloudy (Ackerman et al. 1998).

During dust storms over deserts, the observed AOT values range from 2 to 5 (e.g. Alam et al. 2014). However, over the tropical North Atlantic in July, strong AOT exceeding even 1 is a very rare phenomenon. To demonstrate that AOT exceeding 1 is a rare phenomenon over the tropical North Atlantic, Figure 12(*a*) represents a histogram of AOT observed over the tropical North Atlantic in July 2010, based on MODIS Level 3 AOT daily data. July 2010 was chosen because AOT, averaged over the tropical North Atlantic, was maximal compared to AOT in other July months, during the 10-year study period. One can see that AOT hardly exceeded 1. A similar situation can be seen over the latitudes with SAL presence (12° N–24° N) (Figure 12(*b*)). Therefore, the effect of MODIS CF contamination by heavy dust loading cannot essentially contribute to averaging CF over the tropical North Atlantic. Consequently, given the large amount of available MODIS CF daily data over the 10-year study period, CF contamination does not account for the obtained hemispheric CF asymmetry over the tropical Atlantic Ocean.

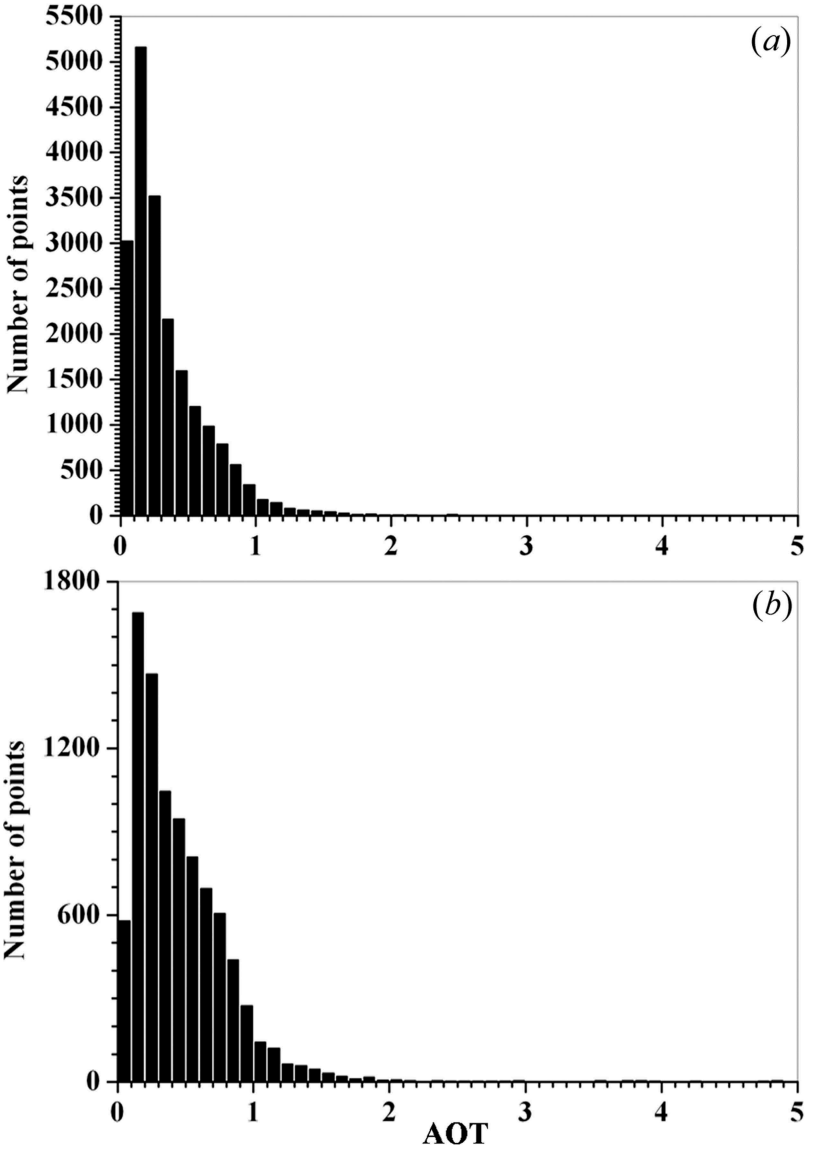

Figure 12. The histogram of AOT observed over the tropical North Atlantic in July 2010, based on Collection 5 MODIS–Terra Level 3 AOT daily data with resolution 1° × 1°: (*a*) over the tropical North Atlantic (30° N–0° N; 60° W–0° E); (*b*) over the latitudes with the SAL presence (12° N–24° N; 60° W–0° E).

5. Conclusions

Meridional distribution of AOT and CF was analysed using 10-year satellite measurements from MISR and MODIS, together with MERRAero data (July 2002–June 2012). In the current study, we focus on the tropical Atlantic (30° N–30° S), which is characterized by significant amounts of Saharan dust dominating other aerosol species over the North Atlantic.

Our main point is that, over the tropical Atlantic, Saharan dust not only is responsible for the pronounced hemispheric aerosol asymmetry, but also contributes to significant cloud cover along the SAL. Over the tropical Atlantic in July, along the SAL, MODIS CF data showed cloud cover up to 0.8–0.9. These CF values are higher than the 10-year mean MODIS CF over the tropical North Atlantic (0.66) (Table 1). This CF along SAL together with clouds over the Atlantic ITCZ contributes to the hemispheric CF asymmetry between the tropical North and South Atlantic. This leads to the imbalance in strong solar radiation, which reaches the sea surface between the tropical North and South Atlantic and, consequently, affects climate formation in the tropical Atlantic.

The observed significant cloud cover along SAL could be explained by the formation of shallow stratocumulus clouds below the temperature inversion with the assistance of settling Saharan dust particles. The temperature inversion at the SAL base prevents deep cloud formation; this explains the limited precipitation of less than 20 mm month^{-1} along SAL (zones 1–4 in Figure 10). In the absence of temperature inversion over the west of the tropical North Atlantic (zones 5 and 6 in Figure 10), one can consider the presence of developed cumulus clouds, which are capable of producing intensive rainfall up to 110 mm month^{-1}.

When hemispheric AOT asymmetry over the tropical North Atlantic was most pronounced, dust AOT averaged separately over the tropical North Atlantic was one order of magnitude higher than that over the tropical South Atlantic. In July, the most pronounced hemispheric asymmetry of dust AOT was characterized by the hemispheric ratio R_{DU} of approximately 30. In the presence of such strong hemispheric asymmetry in dust AOT in the summer months, CF averaged separately over the tropical North Atlantic exceeded CF averaged over the tropical South Atlantic by 20%.

With respect to different oceans, only over the Atlantic Ocean did MERRAero demonstrate that desert dust dominated all other aerosol species and was responsible for hemispheric aerosol asymmetry there. MERRAero showed that, over the tropical Atlantic, dust and carbonaceous aerosols were distributed asymmetrically relative to the equator, whereas other aerosol species were distributed more symmetrically.

Both MISR measurements and MERRAero data were in agreement on seasonal variations in hemispheric aerosol asymmetry. Hemispheric asymmetry in total AOT over the Atlantic was most pronounced between March and July, when dust presence over the North Atlantic was maximal. In September and October, there was no noticeable hemispheric aerosol asymmetry in total AOT over the tropical Atlantic. Over the tropical Atlantic during the season of pronounced hemispheric aerosol asymmetry, we found 20% hemispheric asymmetry in cloud cover, in contrast to the situation over the global ocean. However, during the season with no noticeable hemispheric aerosol asymmetry, we found no noticeable asymmetry in CF.

Acknowledgement

We acknowledge the GES-DISC Interactive Online Visualization and Analysis Infrastructure (Giovanni) for providing us with MODIS and TRMM data.

Disclosure statement

No potential conflict of interest was reported by the authors.

Funding

Dr Long acknowledges support from the Office of Biological and Environmental Research of the US Department of Energy as part of the Atmospheric Systems Research Program. The Tel-Aviv University team acknowledges support from the international Virtual Institute DESERVE (Dead Sea Research Venue), funded by the German Helmholtz Association.

References

Acker, J. G., and G. Leptoukh. 2007. "Online Analysis Enhances Use of NASA Earth Science Data." *Eos, Transactions American Geophysical Union* 88 (2): 14–17. doi:10.1029/2007EO020003.

Ackerman, S. A., K. I. Strabala, W. P. Menzel, R. A. Frey, C. C. Moeller, and L. E. Gumley. 1998. "Discriminating Clear Sky from Clouds with MODIS." *Journal of Geophysical Research* 103 (D24): 32141–32157. doi:10.1029/1998JD200032.

Alam, K., T. Trautmann, T. Blaschke, and F. Subhand. 2014. "Changes in Aerosol Optical Properties Due to Dust Storms in the Middle East and Southwest Asia." *Remote Sensing of Environment* 143: 216–227. doi:10.1016/j.rse.2013.12.021.

Alpert, P., Y. J. Kaufman, Y. Shay-El, D. Tanre, A. da Silva, S. Schubert, and J. H. Joseph. 1998. "Quantification of Dust-Forced Heating of the Lower Troposphere." *Nature* 395: 367–370. doi:10.1038/26456.

Andreae, M. O., D. A. Hegg, and U. Baltensperger. 2009. "Sources and Nature of Atmospheric Aerosols." In *Aerosol Pollution Impact on Precipitation*, edited by Z. Levin and W. R. Cotton, 45–90. Dordrecht: Springer.

Ben-Ami, Y., I. Koren, and O. Altaratz. 2009. "Patterns of North African Dust Transport over the Atlantic: Winter Vs. Summer, Based on CALIPSO first Year Data." *Atmospheric Chemistry and Physics* 9: 7867–7875. doi:10.5194/acp-9-7867-2009.

Chin, M., P. Ginoux, S. Kinne, O. Torres, B. Holben, B. N. Duncan, R. V. Martin, J. Logan, A. Higurashi, and T. Nakajima. 2002. "Tropospheric Aerosol Optical Thickness from the GOCART Model and Comparisons with Satellite and Sun Photometer Measurements." *Journal of the Atmospheric Sciences* 59: 461–483. doi:http://dx.doi.org/10.1175/1520-0469(2002)059<0461:TAOTFT>2.0.CO;2.

Choobari, O. A., P. Zawar-Reza, and A. Sturman. 2014. "The Global Distribution of Mineral Dust and Its Impacts on the Climate System: A Review." *Atmospheric Research* 138: 152–165. doi:10.1016/j.atmosres.2013.11.007.

Chou, M.-D., P.-K. Chan, and M. Wang. 2002. "Aerosol Radiative Forcing Derived from Seawifs-Retrieved Aerosol Optical Properties." *Journal of the Atmospheric Sciences* 59: 748–757. doi:10.1175/1520-0469(2002)059<0748:ARFDFS>2.0.CO;2.

Christopher, S., and J. Wang. 2004. "Intercomparison between Multi-Angle Imaging Spectroradiometer (MISR) and Sunphotometer Aerosol Optical Thickness in Dust Source Regions over China: Implications for Satellite Aerosol Retrievals and Radiative Forcing Calculations." *Tellus B* 56: 451−456. doi:10.3402/tellusb.v56i5.16462.

Colarco, P., A. da Silva, M. Chin, and T. Diehl. 2010. "Online Simulations of Global Aerosol Distributions in the NASA GEOS-4 Model and Comparisons to Satellite and Ground-Based Aerosol Optical Depth." *Journal of Geophysical Research* 115: D14207. doi:10.1029/2009JD012820.

Darmenov, A., and A. da Silva. 2013. "The Quick Fire Emissions Dataset (QFED) - Documentation of Versions 2.1, 2.2 and 2.4." *NASA Technical Report Series on Global Modeling and Data Assimilation. NASA TM-2013-104606*, 32, 183. Greenbelt, MD: NASA.

Diaz, H. F., T. N. Carlson, and J. M. Prospero. 1976. "A Study of the Structure and Dynamics of the Saharan Air Layer over the Northern Equatorial Atlantic during BOMEX." *NOAA Tech Memo ERL WMPO-32*, 61. Silver Spring, MD: NOAA.

Dunion, J. P., and C. S. Velden. 2004. "The Impact of the Saharan Air Layer on Atlantic Tropical Cyclone Activity." *Bulletin of the American Meteorological Society* 85 (3): 353–365. doi:10.1175/BAMS-85-3-353.

Feingold, G., W. Cotton, U. Lohmann, and Z. Levin. 2009. "Effects of Pollution Aerosols and Biomass Burning on Clouds and Precipitation: Numerical Modeling Studies." In *Aerosol*

Pollution Impact on Precipitation, edited by Z. Leven and W. R. Cotton, 243–278. Dordrecht: Springer.

Frey, R. A., S. A. Ackerman, Y. Liu, K. I. Strabala, H. Zhang, J. R. Key, and X. Wang. 2008. "Cloud Detection with MODIS. Part I: Improvements in the MODIS Cloud Mask for Collection 5." *Journal of Atmospheric and Oceanic Technology* 25: 1057–1072. doi:10.1175/2008JTECHA1052.1.

Haywood, J. M., J. Pelon, P. Formenti, N. Bharmal, M. Brooks, G. Capes, P. Chazette, C. Chou, S. Christopher, H. Coe, J. Cuesta, Y. Derimian, K. Desboeufs, G. Greed, M. Harrison, B. Heese, E. J. Highwood, B. Johnson, M. Mallet, B. Marticorena, J. Marsham, S. Milton, G. Myhre, S. R. Osborne, D. J. Parker, J.-L. Rajot, M. Schulz, A. Slingo, D. Tanré, and P. Tulet. 2008. "Overview of the Dust and Biomass-burning Experiment and African Monsoon Multidisciplinary Analysis Special Observing Period-0." *Journal of Geophysical Research* 113: D00C17. doi:10.1029/2008JD010077.

Hsu, N. C., R. Gautam, A. M. Sayer, C. Bettenhausen, C. Li, M. J. Jeong, S.-C. Tsay, and B. Holben. 2012. "Global and Regional Trends of Aerosol Optical Depth over Land and Ocean Using Seawifs Measurements from 1997 to 2010." *Atmospheric Chemistry and Physics* 12: 8037–8053. doi:10.5194/acp-12-8037-2012.

Huffman, G. J., R. F. Adler, D. T. Bolvin, G. Gu, E. J. Nelkin, K. P. Bowman, Y. Hong, E. F. Stocker, and D. B. Wolff. 2007. "The TRMM Multisatellite Precipitation Analysis (TMPA): Quasi-Global, Multiyear, Combined-Sensor Precipitation Estimates at Fine Scales." *Journal of Hydrometeorology* 8: 38–55. doi:10.1175/JHM560.1.

Johnson, B. T., K. P. Shine, and P. M. Forster. 2004. "The Semi-Direct Aerosol Effect: Impact of Absorbing Aerosols on Marine Stratocumulus." *Quarterly Journal of the Royal Meteorological Society* 130: 1407–1422. doi:10.1256/qj.03.61.

Kalashnikova, O. V., and R. Kahn. 2008. "Mineral Dust Plume Evolution over the Atlantic from MISR and MODIS Aerosol Retrievals." *Journal of Geophysical Research* 113: D24204. doi:10.1029/2008JD010083.

Kaufman, Y. J., O. Boucher, D. Tanre, M. Chin, L. A. Remer, and T. Takemura. 2005. "Aerosol Anthropogenic Component Estimated from Satellite Data." *Geophysical Research Letters* 32: L17804. doi:10.1029/2005GL023125.

Kaufman, Y. J., I. Koren, L. Remer, D. Rosenfeld, and Y. Rudich. 2005. "The Effect of Smoke, Dust, and Pollution Aerosol on Shallow Cloud Development over the Atlantic Ocean." *Proceedings of the National Academy of Sciences* 102: 11207–11212. doi:10.1073/pnas.0505191102.

King, M. D., W. P. Menzel, Y. J. Kaufman, D. Tanre, B.-C. Gao, S. Platnick, S. A. Ackerman, L. A. Remer, R. Pincus, and P. A. Hubanks. 2003. "Cloud and Aerosol Properties, Precipitable Water, and Profiles of Temperature and Water Vapor from MODIS." *IEEE Transactions on Geoscience and Remote Sensing* 41 (2): 442–458. doi:10.1109/TGRS.2002.808226.

Kishcha, P., A. M. da Silva, B. Starobinets, and P. Alpert. 2014. "Air Pollution over the Ganges Basin and North-West Bay of Bengal in the Early Post-Monsoon Season Based on NASA Merraero Data." *Journal of Geophysical Research: Atmospheres* 119: 1555–1570. doi:10.1002/2013JD020328.

Kishcha, P., B. Starobinets, and P. Alpert. 2007. "Latitudinal Variations of Cloud and Aerosol Optical Thickness Trends Based on MODIS Satellite Data." *Geophysical Research Letters* 34: L05810. doi:10.1029/2006GL028796.

Kishcha, P., B. Starobinets, O. Kalashnikova, C. N. Long, and P. Alpert. 2009. "Variations of Meridional Aerosol Distribution and Solar Dimming." *Journal of Geophysical Research* 114: D00D14. doi:10.1029/2008JD010975.

Ku, H. 1966. "Notes on the Use of Propagation of Error Formulas." *Journal of Research of National Bureau of Standards – C. Engineering and Instrumentation* 70C (4): 263–273.

Levin, Z., A. Teller, E. Ganor, and Y. Yin. 2005. "On the Interactions of Mineral Dust, Sea-Salt Particles, and Clouds: A Measurement and Modeling Study from the Mediterranean Israeli Dust Experiment Campaign." *Journal of Geophysical Research* 110: D20202. doi:10.1029/2005JD005810.

Lewis, E. R., and S. E. Schwartz. 2004. *Sea Salt Aerosol Production: Mechanisms, Methods, Measurements and Models - A Critical Review*, 413. Washington, DC: AGU.

Liu, Y., J. A. Sarnat, B. A. Coull, P. Koutrakis, and D. J. Jacob. 2004. "Validation of Multiangle Imaging Spectroradiometer (MISR) Aerosol Optical Thickness Measurements Using Aerosol

Robotic Network (AERONET) Observations over the Contiguous United States." *Journal of Geophysical Research* 109: D06205. doi:10.1029/2003JD003981.

Matronchik, J. V., D. J. Diner, R. Kahn, and B. Gaitley. 2004. "Comparison of MISR and AERONET Aerosol Optical Depths over Desert Sites." *Geophysical Research Letters* 31: L16102. doi:10.1029/2004GL019807.

Min, Q.-L., R. Li, B. Lin, E. Joseph, S. Wang, Y. Hu, V. Morris, and F. Chang. 2009. "Evidence of Mineral Dust Altering Cloud Microphysics and Precipitation." *Atmospheric Chemistry and Physics* 9: 3223–3231. doi:10.5194/acp-9-3223-2009.

Mishchenko, M. I., and I. V. Geogdzhayev. 2007. "Satellite Remote Sensing Reveals Regional Tropospheric Aerosol Trends." *Optics Express* 15: 7423–7438. doi:10.1364/OE.15.007423.

NIST/SEMATECH. 2006. "e-Handbook of Statistical Methods." Accessed September 7 2006. http://www.itl.nist.gov/25 div898/handbook/

O'Dowd, C. D., and G. de Leeuw. 2007. "Marine Aerosol Production: A Review of the Current Knowledge." *Philosophical Transactions of the Royal Society A* 365: 1753–1774. doi:10.1098/rsta.2007.2043.

Pey, J., X. Querol, A. Alastuey, F. Forastiere, and M. Stafoggia. 2013. "African Dust Outbreaks over the Mediterranean Basin during 2001–2011: Pm_{10} Concentrations, Phenomenology and Trends, and Its Relation with Synoptic and Mesoscale Meteorology." *Atmospheric Chemistry and Physics* 13: 1395–1410. doi:10.5194/acp-13-1395-2013.

Prospero, J., and T. Carlson. 1972. "Vertical and Areal Distribution of Saharan Dust over the Western Equatorial North Atlantic Ocean." *Journal of Geophysical Research* 77: 5255–5265. doi:10.1029/JC077i027p05255.

Prospero, J., and J. Lamb. 2003. "African Droughts and Dust Transport to the Caribbean: Climate Change Implications." *Science* 302: 1024–1027. doi:10.1126/science.1089915.

Remer, L. A., and Y. J. Kaufman. 2006. "Aerosol Direct Radiative Effect at the Top of the Atmosphere over Cloud Free Ocean Derived from Four Years of MODIS Data." *Atmospheric Chemistry and Physics* 6: 237–253. doi:10.5194/acp-6-237-2006.

Remer, L. A., R. G. Kleidman, R. C. Levy, Y. J. Kaufman, D. Tanré, S. Mattoo, J. V. Martins, C. Ichoku, I. Koren, H. Yu, and B. N. Holben. 2008. "Global Aerosol Climatology from the MODIS Satellite Sensors." *Journal of Geophysical Research* 113: D14S07. doi:10.1029/2007JD009661.

Rosenfeld, D., Y. Rudich, and R. Lahav. 2001. "Desert Dust Suppressing Precipitation: A Possible Desertification Feedback Loop." *Proceedings of the National Academy of Sciences* 98: 5975–5980. doi:10.1073/pnas.101122798.

Tereszchuk, K. A., G. González Abad, C. Clerbaux, D. Hurtmans, P.-F. Coheur, and P. F. Bernath. 2011. "ACE-FTS Measurements of Trace Species in the Characterization of Biomass Burning Plumes." *Atmospheric Chemistry and Physics* 11: 12169–12179. doi:10.5194/acp-11-12169-2011.

Wilcox, E. M., K. M. Lau, and K.-M. Kim. 2010. "A Northward Shift of the North Atlantic Ocean Intertropical Convergence Zone in Response to Summertime Saharan Dust Outbreaks." *Geophysical Research Letters* 37: L04804. doi:10.1029/2009GL041774.

Zhang, J. L., and J. S. Reid. 2010. "A Decadal Regional and Global Trend Analysis of the Aerosol Optical Depth Using A Data-Assimilation Grade Over-Water MODIS and Level 2 MISR Aerosol Products." *Atmospheric Chemistry and Physics* 10: 10949–10963. doi:10.5194/acp-10-10949-2010.